Role of Helix−Helix Interactions in Assembly of the Bacteriorhodopsin Lattice†

Thomas A. Isenbarger and Mark P. Krebs*

Department of Biomolecular Chemistry, University of Wisconsin Medical School, Madison, Wisconsin 53706-1532

Received March 9, 1999; Revised Manuscript Received May 3, 1999

ABSTRACT: The purple membrane of *Halobacterium salinarum* is a two-dimensional lattice of lipids and the integral membrane protein bacteriorhodopsin (BR). To determine whether helix−helix interactions within the membrane core stabilize this complex, we substituted amino acid residues at the helix−helix interface between BR monomers and examined the assembly of the protein into the lattice. Lattice assembly was demonstrated to fit a cooperative self-assembly model that exhibits a critical concentration in vivo. Using this model as the basis for a quantitative assay of lattice stability, bulky substitutions at the helix−helix interface between BR monomers within the membrane core were shown to be destabilizing, probably due to steric clash. Ala substitutions of two residues at the helix−helix interface also reduced stability, suggesting that the side chains of these residues participate in favorable van der Waals packing interactions. However, the stabilizing interactions were restricted to a small region of the interface, and most of the substitutions had little effect. Thus, the contribution of helix−helix interactions to lattice stability appears limited, and favorable interactions between other regions of neighboring BR monomers or between BR and lipid molecules must also contribute.

Many integral membrane proteins must assemble into stable oligomeric complexes to function properly. A long-standing challenge has been to identify and quantify the noncovalent interactions among lipids, proteins, and their prosthetic groups that drive the assembly of these complexes and maintain their stability (*1*−*6*). Due to the unique properties of the membrane, interactions that stabilize membrane protein oligomers may be significantly more complex than those that stabilize water-soluble proteins. These interactions remain poorly understood, in part because of the difficulty of measuring protein association in the lipid bilayer (*4*).

Many studies of membrane protein stability have focused on interactions between transmembrane α-helices, the predominant structural element of integral membrane proteins (*4*). One current model proposes that helix−helix interactions within the membrane contribute significantly to the stability of membrane protein oligomers (*7*). Evidence for this model has been obtained by mutational studies of glycophorin A, which demonstrate that dimerization of its single transmembrane α-helix depends on specific helix−helix interactions. Further support derives from studies of integral membrane proteins of unknown structure that correlate mutations in putative transmembrane helices with defects in function or oligomeric assembly (for reviews, see refs *4* and *5*). Finally, transmembrane helix−helix interactions are clearly apparent in the atomic resolution structures of many membrane protein complexes (*8*−*14*). Although these studies argue that helix−helix interactions contribute to the stability of membrane protein complexes, additional quantitative studies of proteins of known structure are needed to draw general conclusions about the relative importance of these interactions.

Quantitative understanding of membrane protein oligomerization has been difficult for several reasons. First, relatively few structures of membrane protein complexes have been solved at atomic resolution, which is essential for understanding the molecular basis of membrane protein oligomerization. Second, most membrane protein structures have been solved in detergent rather than in a lipid bilayer. Detergent may change protein tertiary structure or induce alternative oligomerization states. Moreover, in detergent the position of proteins with respect to the lipid bilayer cannot be determined. Thus, a mutational study based on the structure of a protein solved in detergent may not faithfully assess the interactions that drive oligomerization in the membrane. Finally, there are few quantitative assays of protein oligomerization in the lipid bilayer. In one approach, transmembrane helices are fused to a reporter domain, such as the DNA-binding domain of ToxR or lambda repressor (*15*−*17*). Reporter activity reflects oligomerization of the transmembrane region in vivo. Although functional assays are improving (*17*), they are indirect and may be influenced by factors such as the depth or orientation of reporter domains within the membrane. The extent of oligomerization measured by functional assays often correlates poorly with independent measures, such as oligomerization on SDS−PAGE (*15*−*17*). Direct determination of protein oligomer-

† This material is based upon work supported under a National Science Foundation Graduate Fellowship to T.A.I. This work was partially funded by a Wisconsin Alumni Research Foundation grant and a Garvin Cremer Scholarship to T.A.I. and Grant MCB 9514280 from the National Science Foundation to M.P.K. This work was also supported in part by a grant to the University of Wisconsin Medical School under the Howard Hughes Medical Institute Research Resources Program for Medical Schools. Circular dichroism data were obtained at the University of Wisconsin−Madison Biophysics Instrumentation Facility, which is supported by the University of Wisconsin−Madison and by Grant BIR-9512577 (NSF).

* To whom correspondence should be addressed. E-mail: mpkrebs@facstaff.wisc.edu. Telephone: (608) 265-5491. Fax: (608) 262-5253.

10.1021/bi9905563 CCC: $18.00
Published on Web 06/19/1999

ization in the lipid bilayer is needed to overcome these difficulties.

To study membrane protein oligomerization, we have chosen the *Halobacterium salinarum* purple membrane, a two-dimensional lattice composed of halobacterial lipids and the seven α-helical transmembrane protein bacteriorhodopsin (BR).[1] The structure of BR has been solved to high resolution in the purple membrane (*18, 19*) and in three-dimensional crystals (*12, 20, 21*). Previous results showed that substitutions of amino acid residues at the BR−BR interface decrease lattice accumulation in vivo (*22*). Here, we quantify the effects of these and other substitutions with a quantitative assay modeled on the cooperative self-assembly of BR. We focused on the assembly of proteins substituted at the helix−helix interface within the hydrocarbon core of the lipid bilayer. The results indicate that interactions within the membrane core contribute to the stability of the BR lattice, but the contribution is small and is unlikely to be solely responsible for the stability of this membrane protein complex.

EXPERIMENTAL PROCEDURES

Materials. Oligonucleotide primers were purchased from Operon Technologies, Inc. (Alameda, CA). Restriction endonucleases were purchased from New England Biolabs, *Pfu* polymerase from Stratagene (La Jolla, CA), and *Taq* polymerase from Promega (Madison, WI). Mevinolin was a generous gift of Dr. A. W. Alberts (Merck, Rahway, NJ). A Perkin-Elmer GeneAmp System 2400 thermocycler was used for PCR. The 1.0 mm quartz capillaries for X-ray powder diffraction were purchased from Charles Supper Co. (Natick, MA).

Selection of Sites for Mutagenesis. Residues targeted for site-directed mutagenesis were originally chosen by analyzing the structural coordinates of BR in 3-dimensional crystals [1ap9 (*12*)]. Using the 1ap9 coordinates, an amino acid residue was selected for mutagenesis if it (i) is present in an α-helical region well within the membrane bilayer, (ii) possesses at least one heavy atom within 4 Å of a heavy atom in the neighboring BR monomer, and (iii) does not possess atoms that interact with loop residues. Subsequent analysis of the other BR structures [1at9 (*19*); 1brr (*20*); 2brd (*18*)] supported the choice of residues. The structures very closely agree in the position and arrangement of the transmembrane α-helices (*12, 19, 20*), which provides a high degree of confidence when defining the helix−helix interface within the membrane core.

Creation of Mutant Strains. Construction of the mutants G113L, I117A, and I117F has been described (*22*). Single substitutions of Ile and Val were created for Gly113, Gly for Ala44, and Ala for the remaining residues. These substitutions were constructed by either standard or two-step "megaprimer" PCR mutagenesis (*23*) in the *Escherichia coli* plasmids pMPK62 (*24*) or its derivative pMPK85, created by ligating the 3.12 kbp *HindIII/SalI* and 5.50 kbp *XhoI/HindIII* fragments from pMPK62. The resulting plasmids carry the mutant bacterioopsin (*bop*) gene and a genetic marker for mevinolin resistance. Mutations at the chromosomal *bop* locus of *H. salinarum* MPK40 were introduced by targeted gene replacement (*24*). Stable strains producing BR were isolated, and Southern analysis confirmed the presence of a single copy of the *bop* gene (*24*). The Perkin-Elmer ABI Prism Dye Terminator kit and AmpliTaq DNA polymerase FS were used in PCR cycle sequencing to confirm the nucleotide sequences of the regions encompassing the PCR products for the *H. salinarum* chromosomal recombinants. Details of primers used and strain construction are available upon request.

Cell Growth and Lysate Preparation. H. salinarum was cultured in liquid media as described (*25*). For critical concentration measurements, saturated cultures were diluted 1:100 or 1:200 in 125 mL Erlenmeyer flasks containing 120 mL of peptone media (*26*) and grown under illumination as described (*22*). Flasks were removed at approximately 10 h intervals starting 35 h after inoculation. After removal, flasks were placed at 4 °C until all could be assayed together; this storage had no effect on BR distribution (data not shown). Cells were harvested by centrifugation at 8000*g* for 30 min in a Sorvall GSA rotor at 4 °C. The supernatant was decanted and the pellet centrifuged briefly to remove residual media. Cells were then suspended in water containing 0.1% NaN_3 and 500 U/ml DNase I (lysis solution) and shaken for 1−1.5 h at room temperature to aid lysis. Cultures from the first three time points were lysed in 2.5 mL of lysis solution, and later cultures were lysed in 3.5 mL. To compensate for low cell density, cultures from two flasks were combined at the first time point.

Determination of BR Distribution. Total protein content in cell lysates was determined by the Micro BCA assay (Pierce, Rockford, IL). Lysates were diluted with water to a total protein concentration of 10 mg/mL, and 1.5 mL of the diluted lysates was applied to 15 mL linear sucrose gradients (38% to 54% w/v) containing 0.025% NaN_3 and 5 mM NaCl. Gradients were spun in a SW-28.1 rotor at 100 000*g* for 17 h at 15 °C. Longer spins do not affect the amount of BR in the lattice fraction, indicating sedimentation equilibrium was achieved. Additionally, sonication of samples did not alter the distribution of BR on the gradients, indicating that the distribution is not influenced by the trapping of lattice material in membrane-derived vesicles formed during cell lysis (J. M. Janz and M.P.K., unpublished results). To fractionate gradients, 65% w/v sucrose was pumped at 1.55 mL/min into the bottom of the gradient tubes and fractions were collected from the top of the gradient through a 250 μL spectrophotometric flow cell. Absorbance was monitored at 570 nm at a rate of 1000 points/s. Using an extinction coefficient of 63 000 M^{-1} cm^{-1} (*27*), the concentration of BR was determined from the integrated absorbance at 570 nm and expressed as a percentage of total cell protein using Microsoft Excel. The concentration of BR in the lattice (BR_l) was plotted versus total BR (BR_t) and fit with the following function to solve for the critical concentration (C_r):

$$BR_t < C_r,\ BR_l = 0 \qquad BR_t \geq C_r,\ BR_l = BR_t - C_r \quad (1)$$

To calculate differences in the Gibbs free energy change of association caused by a substitution ($\Delta\Delta G$), the experimentally determined C_r values were used in the equation

[1] Abbreviations: BR, bacteriorhodopsin; BR_l, lattice BR; BR_t, total BR; λ_{max}, wavelength of maximal absorbance; C_r, critical concentration; ΔΔMS, change in buried molecular surface upon oligomer formation; $\Delta\Delta G$, difference in the Gibbs free energy change.

$$\Delta\Delta G = -RT \ln(C_{r,wt}/C_{r,m}) \quad (2)$$

where $C_{r,wt}$ and $C_{r,m}$ are the C_r values for wild-type and mutant BR, respectively, and a temperature of 298.15 K was used.

Characterization of Purified Proteins. Purple membrane from wild-type and mutant cultures was purified as described (*26*). Absorption spectra were recorded on a Perkin-Elmer Lambda 2 spectrophotometer at room temperature. The 4.7−5.0 μM BR samples in 25 mM sodium phosphate (pH 6.9) were dark-adapted at room temperature for 24 h and light-adapted by illuminating with >520 nm for 5 min. CD spectra were recorded on an Aviv (Lakewood, NJ) 62A DS circular dichroism spectrometer, using a 1 cm quartz microcell and 18 μM BR samples in 25 mM sodium acetate (pH 5.0). Two scans were recorded at 20 °C using a 4 s averaging time, 1 nm bandwidth, and 2 nm sampling interval. A 25 mM sodium acetate solution (pH 5.0) was used as a baseline. Before determination of peak-to-peak heights and zero crossover, CD spectra were smoothed with Igor Pro (WaveMetrics, Inc., Lake Oswego, OR) using a binomial algorithm and smoothing coefficient of 20. For comparison of CD spectra, the extinction coefficients of the mutant BR proteins were assumed to be the same as wild-type, which is reasonable because the mutant and wild-type absorption spectra exhibit a similar ratio of absorbances at 280 and 570 nm. For X-ray analysis, 0.5 mg samples were packed into 1.0 mm quartz capillaries by low-speed centrifugation. Diffraction data were collected on a Histar multiwire detector (Bruker Instruments) with a rotating copper anode X-ray source and double focusing optics. The sample to detector distance was 28.020 cm, accurately calibrated with a Pb_3O_4 diffraction standard. Data were collected for at least 10 min using GADDS powder diffraction software (Bruker Instruments). Diffraction data were integrated using solid angle integration and unwarped using a spatial correction standard. Unwarped peak profiles were analyzed with the freeware application MacDiff 4.0.2 PPC.

Molecular Modeling. Molecular surface calculations were performed on a Silicon Graphics workstation using the MidasPlus interactive molecular display package from the University of California at San Francisco Computer Graphics Laboratory. The *dms* algorithm was used with a probe size of 1.4 Å, dot density of 5 dots/Å^2, and default values for atomic radii. A BR trimer constructed from 1at9 in Sybyl (Tripos, Inc., Saint Louis, MO) was used in the calculations. Mutant monomer and trimer files were created by editing the wild-type PDB coordinate files to remove C_β for A44G and all side chain atoms except C_β for the Ala substitutions. The *dms* algorithm includes implicit hydrogens for carbon, nitrogen, and oxygen atoms.

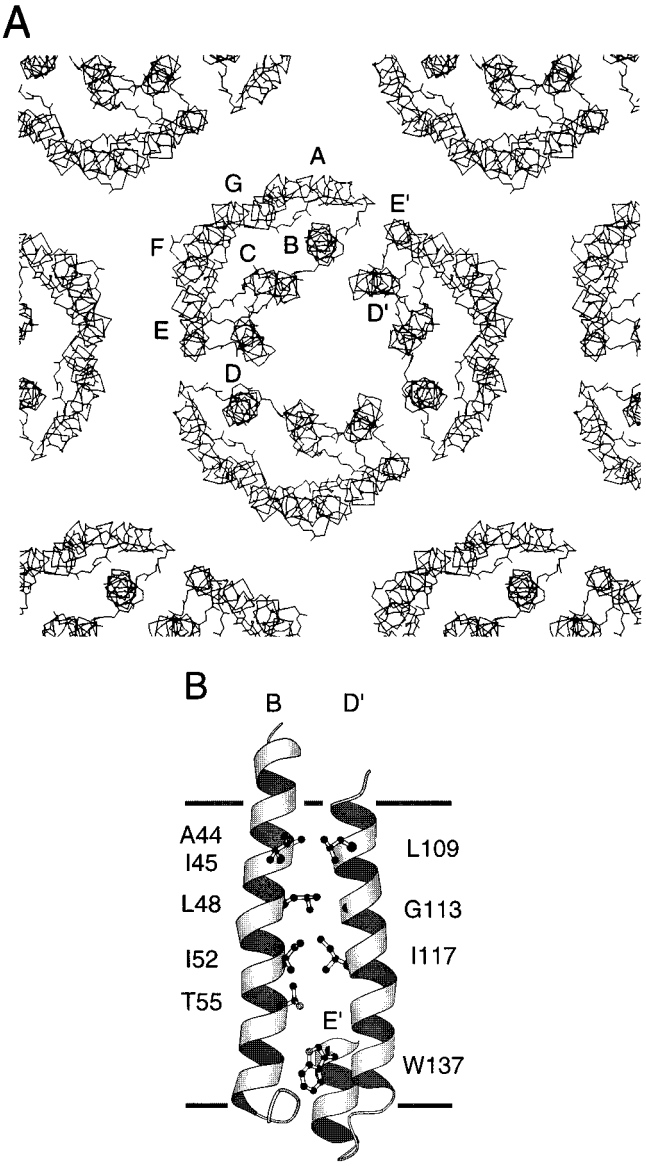

FIGURE 1: (A) Model of the purple membrane lattice. Using the structural coordinates for 1at9 (*19*) obtained from the Brookhaven Protein Data Base, a model of the lattice was constructed in Sybyl (Tripos, Inc., Saint Louis, MO). The polypeptide backbone of each BR monomer is shown perpendicular to the cytoplasmic membrane surface. For the central trimer, helices A−G are denoted for one monomer and D′ and E′ for a neighboring monomer. (B) Interface between transmembrane helices of neighboring BR monomers (ribbons) and residues chosen for substitution (ball-and-stick). The regions of helix B of one BR monomer and helices D′ and E′ of the neighboring monomer that form the BR−BR interface are depicted using MOLSCRIPT (*50*). The view is parallel to the membrane plane as seen from the trimer interior. Horizontal lines denote the boundaries of the membrane core as defined by the lipid ether oxygens derived from the 2brd structure (*18*) when superimposed on the 1at9 structure.

RESULTS

Expression and Characterization of Mutant Proteins. In the BR lattice, the only region of contact between BR monomers occurs at the interface between two monomers within a trimeric unit (Figure 1A). This region of contact encompasses approximately 650 Å^2 of buried surface area (*20*) and includes residues in the membrane core and at the membrane−aqueous boundary. To test if helix−helix interactions within the membrane contribute to the stability of the BR lattice, large and small substitutions of single amino acids were created in this region (Figure 1B). The substitutions were initially designed by analyzing a model of the helix−helix interface within the membrane derived from three-dimensional X-ray crystallographic data (1ap9, see Experimental Procedures). Residues identified from the 1ap9 data were also found in the structure of the native BR lattice obtained by electron crystallography (1at9, Figure 1B). In this work, the 1at9 structure has been used preferentially because of its greater physiological relevance.

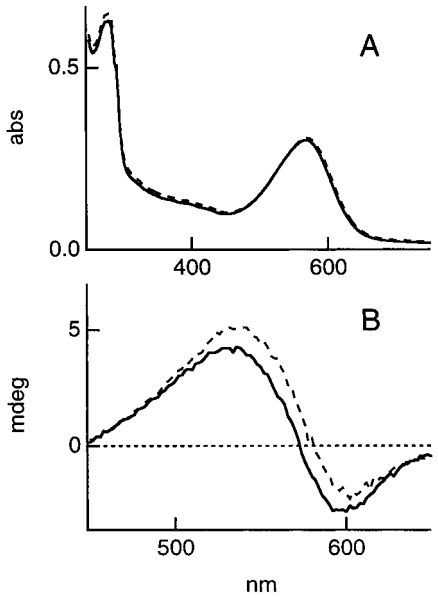

FIGURE 2: Absorption and CD spectra of the purified BR lattice. (A) Wild-type (broken line) and I117A (solid line) were light-adapted for 5 min in light >520 nm. Immediately following illumination, absorption spectra were recorded at room temperature. (B) CD spectra of wild-type (broken line) and I117A (solid line) lattices.

Table 1: Spectroscopic and X-ray Characterization of BR Mutants

	absorbance		circular dichroism		
mutant	DA λ_{max} (nm)	LA λ_{max} (nm)	zero crossover (nm)	peak-to-peak (mdeg)	X-ray unit cell[b] (Å)
A44G	559	569	582	7.4	61.9 ± 0.3
I45A	558	567	579	7.7	61.7 ± 0.3
L48A	558	567	578	8.3	61.8 ± 0.3
I52A	558	567	578	7.9	61.9 ± 0.2
T55A	558	567	582	7.9	61.8 ± 0.3
L109A	559	568	575	8.6	61.8 ± 0.2
G113I	560	571	576	8.8	61.5 ± 0.5
G113L	557[a]	567[a]	577	6.5	62.9 ± 0.4[c]
G113V	560	571	577	8.8	61.8 ± 0.4
I117A	558[a]	566[a]	573	8.8	61.7 ± 0.4
I117F	557[a]	564[a]	574	7.4	61.7 ± 0.4
wild-type	560	568	578 ± 4.1	7.6	61.8 ± 0.4

[a] Values reported previously (*22*). [b] Mean and standard deviation of the unit cell dimensions calculated from a single sample. Analysis of multiple samples reduces the error to ≈0.1. [c] Value was determined after recalibration of sample-to-detector distance and was within 0.1 Å of the wild-type value.

BR mutants substituted at the helix−helix interface between neighboring BR monomers (Figure 1B) were expressed in *H. salinarum* by recombining mutant *bop* gene constructs into the chromosome. Except for W137A, the mutant BR proteins were expressed to within 75−90% of wild-type BR as determined by SDS−PAGE and by the absorbance of BR-containing gradient fractions (data not shown). The purified lattice form of the mutant proteins was examined by UV/visible absorption spectroscopy; a typical result is shown in Figure 2A. Apart from W137A, each of the mutant proteins exhibited normal light- and dark-adapted spectral properties, with an absorption maximum within 4 nm of the value for wild-type BR (Table 1). This is consistent with a normal tertiary fold, although subtle changes in structure would not necessarily be detected by this method. W137A was expressed at approximately 10% of the wild-type level, did not form a recoverable lattice fraction, and had an altered UV/visible absorption spectrum. The structure of this protein is probably abnormal and it was not studied further.

Circular dichroism (CD) spectroscopy and low-angle X-ray diffraction were used to characterize the lattice form of the mutant proteins. The bilobed CD spectrum of the wild-type lattice is thought to result from exciton coupling among ordered BR molecules (*28*). The CD spectra recorded for the wild-type lattice and a representative mutant are shown in Figure 2B. The CD spectra for all the mutants were bilobed and had peak-to-peak heights within 15% of wild-type and zero crossover wavelengths within 5 nm (Table 1). Thus, the spectra are very similar given the considerable noise inherent in the method. The structure of the purified lattices was also examined by X-ray diffraction. The mutant and wild-type lattices diffracted to ∼7 Å, and all were organized in a hexagonal lattice with the same space group (P_3) and unit cell dimensions (Table 1). Taken together, the absorption, CD, and X-ray data demonstrate that the substitutions in BR do not significantly alter retinal binding or the structure of the assembled lattice.

Critical Concentration Assay for BR Assembly. To compare the effects of the substitutions on lattice stability, we developed a quantitative assay of BR association. Because the purple membrane is a two-dimensional crystal, its accumulation may be modeled as a cooperative self-assembly process as described for other protein polymers (*29*, *30*). A hallmark of cooperative self-assembly is the critical concentration (C_r). C_r is the minimal concentration of total protomer required to initiate formation of the polymer and is equivalent to $1/K_{app}$, where K_{app} is the apparent equilibrium constant for addition of protomers to the assembly (*30*). In the case of BR, K_{app} applies to the overall process $n\text{BR} \leftrightarrow \text{BR}_n$, where BR represents the monomer and BR_n the lattice. This model does not discriminate between direct addition of the monomer to the lattice and formation of intermediates such as BR dimers or trimers. In cooperative self-assembly such kinetic intermediates are present at low concentrations and do not influence K_{app}. Mutants that disrupt the lattice, such as I117A (*22*), are expected to exhibit a lower K_{app} and a higher C_r than wild-type BR.

To test the self-assembly model, we measured the amounts of wild-type and I117A BR present in the purple membrane lattice as a function of total cellular BR. Because BR expression is induced in illuminated anaerobic cultures, it was possible to prepare samples containing increasing amounts of BR per cell by harvesting cultures at various times during induction. Total BR and the fraction in the lattice form were quantified by fractionating cell lysates on sucrose gradients and then determining BR content by absorption spectroscopy. The lattice fraction increases as total BR increases but only after a minimal concentration of BR accumulates (Figure 3A), consistent with cooperative self-assembly (*29*). Graphical treatment of the data (Figure 3B) confirms the self-assembly model and demonstrates an increase in C_r for I117A as predicted. C_r thus provides a quantitative measure of lattice stability that is independent of the BR level in any particular culture being examined and can be used to compare the effects of substitutions on lattice stability.

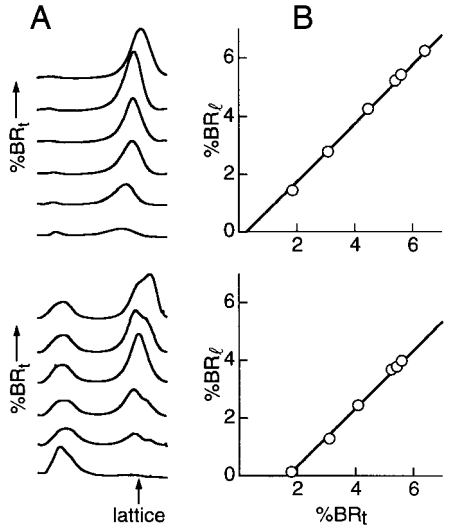

FIGURE 3: Distribution of BR as a function of total cellular BR. (A) Flow cell traces. Wild-type (top) and I117A (bottom) cell lysates containing increasing BR were applied to sucrose density gradients and centrifuged to equilibrium; the trace corresponding to the lowest BR level is shown at the bottom of each series. Gradients were collected from the top through a spectrophotometric flow cell, and absorbance was monitored at 570 nm. Absorbance in each trace is plotted as a function of time. (B) The concentration of BR in the lattice was graphed against total BR for wild-type (top) and I117A (bottom). The data were fit with eq 1 to determine the C_r values for wild-type and I117A lattices. BR concentrations are expressed as a weight percentage of total cellular protein.

The wild-type C_r value is very low, which reflects the high stability of the wild-type purple membrane (Figure 4 and Table 2). Very little of the low-density form of wild-type BR is observed, suggesting that monomers and possible intermediate forms are not abundant. The small amount of the low-density form of wild-type BR is obscured by other pigments that comigrate with the protein. Consequently, the value of C_r presented for wild-type (Table 2) should be considered an upper limit of C_r for this protein.

For analysis of mutant proteins by the self-assembly model, several criteria must be met regarding assembly of BR in the *H. salinarum* membrane. First, the model requires that equilibrium conditions apply. This requirement was tested by growing multiple cultures of L48A to the same density, simultaneously removing them from incubation, and allowing each to sit for 0, 2, or 4 days before preparing lysates. After centrifugation, the same distribution of lattice BR was found for all samples, indicating that equilibrium had been reached (data not shown). Moreover, in vitro studies have demonstrated an equilibrium between BR monomers and aggregates in a lipid bilayer (*31*), supporting our assumption. Second, the model requires that molecular crowding effects that may hinder membrane protein diffusion within the *H. salinarum* membrane are minimal. That the model is valid at high BR concentrations suggests that departures from ideal behavior caused by such effects are negligible. Third, to allow comparison of wild-type and mutant BR C_r values, it is assumed that the ratio between cell membrane surface area and total cellular protein is similar for both types of cells. This is reasonable, as cells are induced in stationary phase when few changes in cell dimension or total protein levels are expected.

Measure of Self-Assembly in Wild-Type and BR Mutants. To determine if residues at the helix−helix interface are important for BR lattice stability, the self-assembly assay was used to examine the stability of the wild-type and mutant BR proteins substituted at the helix−helix interface (Figure 4). All the mutant proteins fit the self-assembly model and thus could be assigned a C_r value. Bulky substitutions of Gly113 all caused large increases in C_r, and the substitution of Phe for Ile117 caused a modest increase in C_r. Substitution

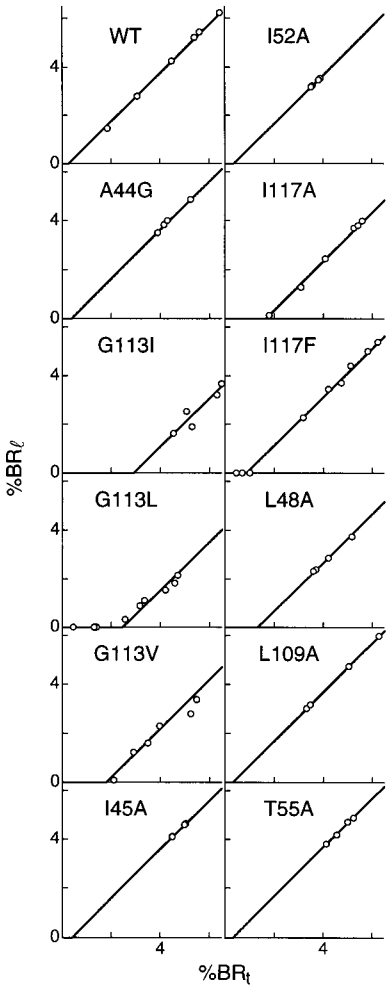

FIGURE 4: Self-assembly assay of wild-type and mutant BR. All mutants substituted at the helix−helix interface were assayed as described in Figure 3B and their C_r values determined by fitting to the self-assembly model.

Table 2: Critical Concentration Values of Bacteriorhodopsin Mutants

mutant	C_r
wild-type	0.24 ± 0.04[a]
large substitutions	
G113I	2.94 ± 0.14
G113L	2.45 ± 0.09
G113V	1.96 ± 0.12
I117F	0.83 ± 0.05
small substitutions	
A44G	0.34 ± 0.02
I45A	0.39 ± 0.01
L48A	1.32 ± 0.03
I52A	0.35 ± 0.01
T55A	0.34 ± 0.02
L109A	0.29 ± 0.01
I117A	1.65 ± 0.03

[a] BR concentrations are expressed as a weight percentage of total protein and errors are the standard errors as described in ref *49*.

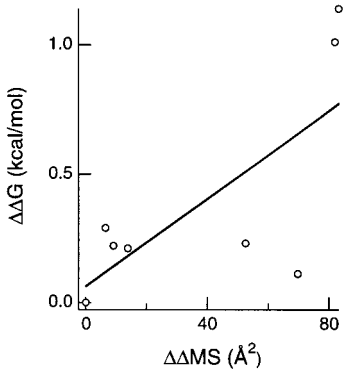

FIGURE 5: $\Delta\Delta G$ versus $\Delta\Delta$MS. For each of the small substitutions, $\Delta\Delta G$ was calculated from the experimentally determined C_r and eq 2. The resulting values are plotted against the $\Delta\Delta$MS values calculated from the 1at9 trimer.

of residues with smaller side chains were generally less disruptive; these substitutions only generated significant increases in C_r at two positions, Leu48 and Ile117 (Table 2).

Calculated Effects of BR Substitutions. To evaluate the molecular basis of lattice stability conferred by the helix−helix interface, we have attempted to estimate the free energy change of lattice formation and correlate it with the surface area buried at the helix−helix interface. Using eq 2, the C_r values of wild-type and mutant proteins can be used to derive the $\Delta\Delta G$ caused by a substitution. For the Ala and Gly substitutions, $\Delta\Delta G$ was compared with the change in buried molecular surface area upon oligomerization ($\Delta\Delta$MS), which provides a crude estimate of the change in van der Waals contacts between BR monomers. The attempt to correlate $\Delta\Delta$MS with $\Delta\Delta G$ is valid despite the uncertainty in the wild-type C_r because each mutant value is computed relative to the same wild-type value. The $\Delta\Delta$MS correlates very poorly ($r^2 = 0.52$) with $\Delta\Delta G$ (Figure 5). Similar results were obtained with other trimer models (data not shown). This suggests that a mathematical model of BR oligomerization must include factors besides the van der Waals interaction of residues at the helix−helix interface.

DISCUSSION

We have used a cooperative self-assembly model of BR assembly to develop a quantitative assay for purple membrane lattice stability. The self-assembly model provides a direct measure of lattice stability, C_r, which can be used to compare the stabilities of wild-type and mutant BR complexes. Using this assay, we examined a series of amino acid substitutions in BR to test the model that helix−helix interactions within the membrane core stabilize membrane protein complexes. Both large and small substitutions were examined. Spectrometric and X-ray diffraction measurements suggest that these substitutions have minimal effects on BR structure.

Bulky substitutions of Gly113 and Ile117 increase C_r, indicating a decrease in lattice stability. This is likely due to steric clash with residues on the opposing helix, since the side chain of Leu48 packs onto Gly113 according to the structural models. Alternatively, the larger side chain may clash sterically with lipids known to be present in the trimer interior (*18*, *20*, *32*). A rough correlation exists between the increase in C_r (G113I > G113L > G113V > I117F) and the relative increase in side chain volume introduced by these bulky substitutions (G113I = G113L > G113V > I117F). These experiments suggest that the BR helix−helix interface is tightly packed, such that little space exists to accommodate extra side chain volume. This supports findings that the density of protein−protein interfaces within the membrane is similar to the tightly packed apolar cores of soluble proteins (*4*) and that the close packing of transmembrane helices contributes to the stability of membrane protein oligomers (*33*−*36*).

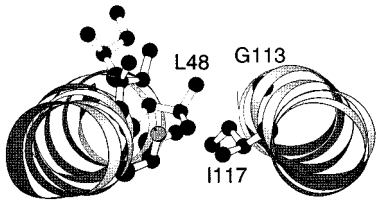

FIGURE 6: View of the helix−helix interface as seen from the cell exterior. Helices are drawn as ribbons with residues at the helix−helix interface represented by sticks. MOLSCRIPT (*50*) and the 1at9 structural coordinates were used for this drawing. Labeled residues indicate those positions where substitutions cause significant increases in C_r.

Replacement of Leu48 and Ile117 with a smaller amino acid, Ala, increases C_r substantially, while substitution of other residues at the helix−helix interface with Ala or Gly increase C_r only slightly. The simplest interpretation of these results is that Leu48 and Ile117 participate in favorable side chain contacts important for lattice stability, whereas the other residues contribute little to stability. The localization of stabilizing interactions to a small cluster of side chains at the helix−helix interface is similar to the localization of important contacts to small dimerization motifs of membrane proteins (*37*) or to "hot spots" at the highly apolar dimer interfaces of soluble proteins (*38*, *39*). Overall, these results support the model that helix−helix interactions contribute at least in part to the stability of membrane protein complexes. They also suggest that van der Waals contacts involving nonpolar amino acids within the membrane core are important for membrane protein association and stability.

Our results show that the change in buried molecular surface area upon lattice formation ($\Delta\Delta$MS) is poorly correlated with lattice destabilization (Figure 5). L48A and I117A show the largest $\Delta\Delta$MS values, suggesting that Leu48 and Ile117 are well-buried at the helix−helix interface. This is readily apparent from the trimer structural model, in which these residues appear to bridge the interface (Figure 6). Thus, Leu48 and Ile117 may contribute a large surface area for favorable association via van der Waals close-packing interactions (Figure 6), resulting in substantial changes in ΔG upon substitution. However, L109A also shows a large $\Delta\Delta$MS but has a small $\Delta\Delta G$. This indicates that factors other than favorable van der Waals interactions must be considered. Changes in side chain or lipid entropy undoubtedly affect the stability of membrane protein complexes (*40*, *41*), but these effects are as yet poorly understood and difficult to model accurately.

Our results suggest that the contribution of helix−helix interactions to BR lattice stability is surprisingly small. Using the wild-type C_r as an upper limit, we calculate that Leu48 and Ile117 each contribute no more than ~1.0 kcal/mol to the stability of the BR lattice and the other residues tested

make a considerably less significant contribution of 0.1−0.3 kcal/mol. It seems likely that other residues may contribute significantly to the stability of the purple membrane lattice. For example, Trp137 makes several contacts with the neighboring BR monomer at the helix−helix interface. Unfortunately, the role of Trp137 cannot be tested by Ala substitution because W137A appears to have an altered monomer structure. Favorable interactions at the membrane−aqueous boundary may also contribute, as suggested for other membrane protein complexes (*3*, *42*−*44*). In support of this, a substitution of Ala for Tyr64, a residue at the membrane boundary, is as destabilizing as bulky substitutions within the membrane core (T.A.I. and M.P.K., unpublished results). Finally, protein−lipid interactions may play a major role in stabilizing the BR lattice, as suggested by BR assembly studies in vitro (*45*, *46*) and evidence of critical BR−lipid contacts in structural analyses (*18*, *20*, *32*).

Another possible explanation for the small effects of the substitutions is that subtle structural changes compensate for the energetic effects of the substitutions. The substitutions may cause undetected structural changes elsewhere in the BR monomer that offset the effects of substitution at the helix−helix interface. Alternatively, the substitutions may allow a change in the organization of lipid or water molecules that balances the loss of favorable contacts in the mutant proteins. An increase in lipid motion or a disordering of water molecules could result in the same type of entropy−enthalpy compensation reported in studies of soluble protein oligomers (*47*, *48*). Structural studies at high resolution are needed to resolve these issues.

CONCLUSION

The assembly of the BR lattice in vivo is a cooperative process and can be described by a self-assembly model. By employing this model in an assay of BR lattice stability, we have shown that the helix−helix interface between BR monomers is tightly packed and that Leu48 and Ile117 are involved in stabilizing the lattice. However, because only two side chains can be demonstrated to be important for stability, it is unlikely that helix−helix interactions are sufficient for BR lattice stability. Attempts to correlate the assembly phenotype with changes in the surface area buried upon oligomerization suggest that factors other than van der Waals packing are likely to have significant roles in lattice stability.

ACKNOWLEDGMENT

We thank Darrell McCaslin and Ivan Rayment for assistance in the collection and analysis of circular dichroism and X-ray diffraction data, respectively. We also thank Milo Westler for help with molecular surface calculations, Eva Pebay-Peyroula for access to structural coordinates before public release, and Oleg Tsodikov and Tom Record for helpful discussions of self-assembly thermodynamics. We thank Heather L. Dale, Ron F. Peck, and Christine M. Angevine for their comments in preparation of the manuscript and Jay M. Janz for technical help.

REFERENCES

1. Gennis, R. B. (1989) *Biomembranes: Molecular Structure and Function*, Springer-Verlag, New York.
2. Haltia, T., and Freire, E. (1995) *Biochim. Biophys. Acta 1241*, 295−322.
3. Cramer, W. A., Engelman, D. M., von Heijne, G., and Rees, D. C. (1992) *FASEB J. 6*, 3397−3402.
4. Lemmon, M. A., MacKenzie, K. R., Arkin, I. T., and Engelman, D. M. (1997) in *Membrane Protein Assembly* (von Heijne, G., Ed.) pp 3−23, Chapman & Hall, New York.
5. Bormann, B. J., and Engelman, D. M. (1992) *Annu. Rev. Biophys. Biomol. Struct. 21*, 223−242.
6. Yeates, T. (1993) in *Thermodynamics of Membrane Receptors and Channels* (Jackson, M. B., Ed.) pp 1−25, CRC Press, Boca Raton, FL.
7. Popot, J. L., and Engelman, D. M. (1990) *Biochemistry 29*, 4031−4037.
8. Deisenhofer, J., Epp, O., Miki, K., Huber, R., and Michel, H. (1985) *Nature 318*, 618−624.
9. Kühlbrandt, W., Wang, D. N., and Fujiyoshi, Y. (1994) *Nature 367*, 614−621.
10. Iwata, S., Ostermeier, C., Ludwig, B., and Michel, H. (1995) *Nature 376*, 660−669.
11. Tsukihara, T., Aoyama, H., Yamashita, E., Tomizaki, T., Yamaguchi, H., Shinzawa-Itoh, K., Nakashima, R., Yaono, R., and Yoshikawa, S. (1996) *Science 272*, 1136−1144.
12. Pebay-Peyroula, E., Rummel, G., Rosenbusch, J. P., and Landau, E. M. (1997) *Science 277*, 1676−1681.
13. Doyle, D. A., Cabral, J. M., Pfuetzner, R. A., Kuo, A., Gulbis, J. M., Cohen, S. L., Chait, B. T., and MacKinnon, R. (1998) *Science 280*, 69−77.
14. Chang, G., Spencer, R. H., Lee, A. T., Barclay, M. T., and Rees, D. C. (1998) *Science 282*, 2220−2226.
15. Leeds, J. A., and Beckwith, J. (1998) *J. Mol. Biol. 280*, 799−810.
16. Langosch, D., Brosig, B., Kolmar, H., and Fritz, H. J. (1996) *J. Mol. Biol. 263*, 525−530.
17. Russ, W. P., and Engelman, D. M. (1999) *Proc. Natl. Acad. Sci. U.S.A. 96*, 863−868.
18. Grigorieff, N., Ceska, T. A., Downing, K. H., Baldwin, J. M., and Henderson, R. (1996) *J. Mol. Biol. 259*, 393−421.
19. Kimura, Y., Vassylyev, D. G., Miyazawa, A., Kidera, A., Matsushima, M., Mitsuoka, K., Murata, K., Hirai, T., and Fujiyoshi, Y. (1997) *Nature 389*, 206−211.
20. Essen, L.-O., Siegert, R., Lehmann, W. D., Oesterhelt, D. (1998) *Proc. Natl. Acad. Sci. U.S.A. 95*, 11673−11678.
21. Luecke, H., Richter, H. T., and Lanyi, J. K. (1998) *Science 280*, 1934−1937.
22. Krebs, M. P., Li, W., and Halambeck, T. P. (1997) *J. Mol. Biol. 267*, 172−183.
23. White, B. A. (1997) *Methods Mol. Biol. 67*, 173−182.
24. Krebs, M. P., Mollaaghababa, R., and Khorana, H. G. (1993) *Proc. Natl. Acad. Sci. U.S.A. 90*, 1987−1991.
25. Cline, S. W., and Doolittle, W. F. (1987) *J. Bacteriol. 169*, 1341−1344.
26. Oesterhelt, D., and Stoeckenius, W. (1974) *Methods Enzymol. 31*, 667−678.
27. Rehorek, M., and Heyn, M. P. (1979) *Biochemistry 18*, 4977−4983.
28. Cassim, J. Y. (1992) *Biophys. J. 63*, 1432−1442.
29. Oosawa, F., and Kasai, M. (1962) *J. Mol. Biol. 4*, 10−21.
30. Andreu, J. M., and Timasheff, S. N. (1986) *Methods Enzymol. 130*, 47−59.
31. Gulik-Krzywicki, T., Seigneuret, M., and Rigaud, J. L. (1987) *J. Biol. Chem. 262*, 15580−15588.
32. Weik, M., Patzelt, H., Zaccai, G., and Oesterhelt, D. (1998) *Mol. Cell 1*, 411−419.
33. Arkin, I. T., Adams, P. D., MacKenzie, K. R., Lemmon, M. A., Brunger, A. T., and Engelman, D. M. (1994) *EMBO J. 13*, 4757−4764.
34. Patricelli, M. P., Lashuel, H. A., Giang, D. K., Kelly, J. K., and Cravatt, B. F. (1998) *Biochemistry 37*, 15177−15187.
35. Lemmon, M. A., Flanagan, J. M., Hunt, J. F., Adair, B. D., Bormann, B. J., Dempsey, C. E., and Engelman, D. M. (1992) *J. Biol. Chem. 267*, 7683−7689.
36. Lemmon, M. A., Flanagan, J. M., Treutlein, H. R., Zhang, J., and Engelman, D. M. (1992) *Biochemistry 31*, 12719−12725.

37. Lemmon, M. A., Treutlein, H. R., Adams, P. D., Brunger, A. T., and Engelman, D. M. (1994) *Nat. Struct. Biol. 1*, 157−163.
38. Bogan, A. A., and Thorn, K. S. (1998) *J. Mol. Biol. 280*, 1−9.
39. Dall'Acqua, W., Goldman, E. R., Lin, W., Teng, C., Tsuchiya, D., Li, H., Ysern, X., Braden, B. C., Li, Y., Smith-Gill, S. J., and Mariuzza, R. A. (1998) *Biochemistry 37*, 7981−7991.
40. MacKenzie, K. R., and Engelman, D. M. (1998) *Proc. Natl. Acad. Sci. U.S.A. 95*, 3583−3590.
41. Jähnig, F. (1983) *Proc. Natl. Acad. Sci. U.S.A. 80*, 3691−3695.
42. Verrall, S., and Hall, Z. W. (1992) *Cell 68*, 23−31.
43. Phale, P. S., Philippsen, A., Kiefhaber, T., Koebnik, R., Phale, V. P., Schirmer, T., and Rosenbusch, J. P. (1998) *Biochemistry 37*, 15663−15670.
44. Schiffer, M., Chang, C. H., and Stevens, F. J. (1992) *Protein Eng. 5*, 213−214.
45. Sternberg, B., L'Hostis, C., Whiteway, C. A., and Watts, A. (1992) *Biochim. Biophys. Acta 1108*, 21−30.
46. Watts, A. (1995) *Biophys. Chem. 55*, 137−151.
47. Pearce, K. H., Jr., Ultsch, M. H., Kelley, R. F., de Vos, A. M., and Wells, J. A. (1996) *Biochemistry 35*, 10300−10307.
48. Brummell, D. A., Sharma, V. P., Anand, N. N., Bilous, D., Dubuc, G., Michniewicz, J., MacKenzie, C. R., Sadowska, J., Sigurskjold, B. W., Sinnott, B., Young, N. M., Bundle, D. R., and Narang, S. A. (1993) *Biochemistry 32*, 1180−1187.
49. Fletcher, R. (1980) *Practical Methods of Optimization*, Vol. 1, Wiley, New York.
50. Kraulis, P. (1991) *J. Appl. Crystallogr. 24*, 946−950.

BI9905563